ACS APPLIED MATERIALS & INTERFACES

www.acsami.org

Forum Article

4D Printable Tough and Thermoresponsive Hydrogels

Mutian Hua,[†] Dong Wu,[†] Shuwang Wu, Yanfei Ma, Yousif Alsaid, and Ximin He*

Cite This: https://dx.doi.org/10.1021/acsami.0c17532

Read Online

ACCESS | Metrics & More | Article Recommendations | Supporting Information

ABSTRACT: Hydrogels with attractive stimuli-responsive volume changing abilities are seeing emerging applications as soft actuators and robots. However, many hydrogels are intrinsically soft and fragile for tolerating mechanical damage in real world applications and could not deliver high actuation force because of the mechanical weakness of the porous polymer network. Conventional tough hydrogels, fabricated by forming double networks, dual cross-linking, and compositing, could not satisfy both high toughness and high stimuli responsiveness. Herein, we present a material design of combining responsive and tough components in a single hydrogel network, which enables the synergistic realization of high toughness and actuation performance. We showcased this material design in an exemplary tough and thermally responsive hydrogel based on PVA/(PVA-MA)-*g*-PNIPAM, which achieved 100 times higher toughness (~10 MJ/m^3) and 20 times higher actuation stress (~10 kPa) compared to conventional PNIPAM hydrogels, and a contraction ratio of up to 50% simultaneously. The effects of salt concentration, polymer ratio, and structural design on the mechanical and actuation properties have been systematically investigated. Utilizing 4D printing, actuators of various geometries were fabricated, as well as lattice-architected hydrogels with macro-voids, presenting 4 times faster actuation speed compared to bulk hydrogel, in addition to the high toughness, actuation force, and contraction ratio.

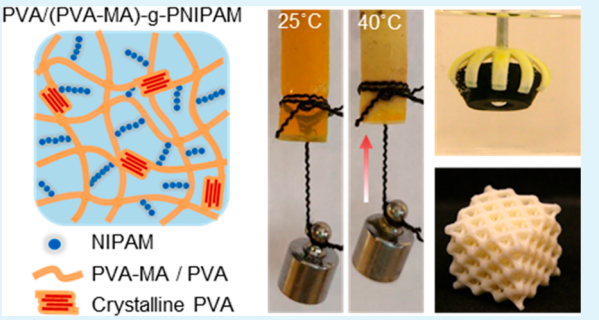

KEYWORDS: *4D printing, hydrogel actuator, tough hydrogel, salting out, thermoresponsive hydrogel, photoresponsive hydrogel*

INTRODUCTION

Stimuli-responsive hydrogels are widely used for soft actuators and soft robots because of their facile fabrication, diverse actuation modes, and high degree of freedom during actuation.[1] Hydrogel actuators are seeing growing interests as underwater robots and biomedical tools in light of their excellent compatibility with aqueous and biological environment.[2−6] Among various stimuli-responsive polymeric actuators, thermoresponsive ones have attracted particular interest due to the easy induction of thermal energy in the material without compositional change to the system.[7,8] Poly(*N*-isopropylacrylamide) (PNIPAM) hydrogels are a representative example that exhibit distinct behaviors at temperatures above or below their lower critical solution temperature (LCST).[9] PNIPAM hydrogels absorb water and swell at a temperature below LCST and conversely expel water and shrink at temperature above LCST. PNIPAM-based actuators have shown significant advantages over many other types of hydrogels because of remote powering and control capabilities when conjugated with photothermal/magnetothermal materials.[4,6,10]

Conventional hydrogels, especially PNIAPM hydrogels, are mechanically weak because of their low solid contents (70−98% water contents) and lack of energy dissipating mechanisms.[11−15] Their intrinsic softness and fragileness lead to low deliverable force[16,17] and large passive deformation upon contact when applied as actuators, which hinders their use in practical applications that involve high loads, abrupt impacts, and long-term services. Various methods such as forming double networks (DN),[12,18] having dual cross-linking,[19] and compositing[20−25] were introduced for toughening hydrogels. However, many tough hydrogels are incapable of actuation by ambient stimuli while maintaining high toughness because of the consumption of stimuli-responsive sites or immobilization by the secondary networks or stiff fillers during the toughening process. For PNIPAM hydrogels, some viable approaches utilized solvent exchanges that induced strong aggregation or collapse of polymer chains for combined strengthening and actuation.[26−33] These methods require replenishing the entire body of solvent for reverse actuation and therefore limit the working environment of actuators to finite-sized containers. Alternatively, electro-actuation and pneumatic/hydraulic actuation have been employed to actuate tough hydrogels,[5,34,35] which requires external powering and pumping systems to supply sufficient voltage or pressure.

Special Issue: Novel Stimuli-Responsive Materials for 3D Printing

Received: September 29, 2020
Accepted: November 19, 2020

Achieving high mechanical robustness and stimuli responsiveness simultaneously has been difficult for hydrogels. Many toughening methods that involve addition of secondary networks,[18] cross-linkers,[12] or reinforcements[23,24] are incompatible for building tough and stimuli-responsive actuators, as the stimuli-responsive network is internally restrained by the nonresponsive toughening components. Some water-free polymer systems are easily made to be tough and stimuli responsive, like liquid crystal elastomers (LCEs)[36,37] and poly(pyrrole).[38] These materials consist of tough polymer backbones and stimuli-responsive functional groups in a single network. Therefore, it would be advantageous to synthesize hydrogels with an intrinsically tough and stimuli-responsive network to realize simultaneous high toughness and stimuli responsiveness.

Herein, we present a tough and responsive hydrogel synthesized by grafting stimuli-responsive monomers to polymers with high toughness. Poly(vinyl alcohol) (PVA) is a high-molecular-weight polymer with excellent mechanical properties due to its high fracture toughness compared to the short chain counterparts.[39] PVA also has a good ability to form nanocrystalline domains for further strengthening and toughening the network via post treatments.[40,41] Therefore, we used PVA and its methacrylate derivatives (PVA-MA) as the tough polymer backbone. The modification from PVA to PVA-MA enabled the photo polymerization of this tough polymer. In this study, *N*-isopropylacrylamide (NIPAM) was used as an exemplary responsive monomer for grafting onto the PVA-MA backbone to give PVA thermoresponsiveness and PVA/(PVA-MA)-*g*-PNIPAM hydrogel was fabricated via digital light processing (DLP)-based 4D printing.[42] A facile salting out treatment was used subsequently to induce the formation of PVA nanocrystalline domains to further strengthen the hydrogel network. The printed hydrogels showed exceptionally high strength, high toughness, good thermoresponsiveness, and improved actuation force, and they are highly tunable because of the ability to spatially program the material properties by 4D printing. The presented tough and responsive hydrogel system, with its simple synthesis and modular design, holds great potential for constructing tough and high-power soft robots, biomedical devices, and hydrogel actuators.

MATERIALS AND METHODS

Materials. Poly(vinyl alcohol) (PVA, 99% hydrolyzed, MW 89 000−98 000), *N*-isopropylacrylamide (NIPAM, 99%), methacrylic acid (MA, 99%), *N*,*N*′-methylenebis(acrylamide) (Bis), 2-hydroxy-4′-(2-hydroxyethoxy)-2-methylpropiophenone (Irgacure 2959), tartrazine, and hydroquinone were purchased from Sigma-Aldrich. Lithium phenyl-2,4,6-trimethylbenzoylphosphinate (TPO-Li) was purchased from CPS Polymers. Hexane, hydrochloric acid, acetone, and triethyl amine were purchased from Fisher Scientifics. NIPAM was purified by recrystallization in hexane. All other chemicals were used without further treatment.

Synthesis of PVA-MA. The PVA-MA was synthesized by a condensation reaction between PVA and MA (Figure S1A). Typically, 20 g of PVA was dissolved in 180 mL of DI water in a conical flask with heating. Forty milligrams of hydroquinone was added to the solution. After cooling down, 5 mL of MA and 10 mL of hydrochloric acid was added to the solution. The mixture was stirred at 300 rpm and 60 °C for 12 h. After cooling down, 15 mL of triethyl amine was added to the solution. The whole solution was then diluted 10 times and precipitated in acetone. The precipitate was finally filtered and dried in a vacuum.

Preparation of Printing Precursor. The printing precursor consists of $(10 - x)$ wt % PVA, x wt % PVA-MA, 20 wt % NIPAM, and 0.1 wt % TPO-Li dissolved in water. The hydrogels were denoted as "xP-MA_$(10 - x)$P" for x wt % PVA-MA added in the total precursor. For controlling light penetration depth, 0.2 wt % tartrazine as photoabsorber was added to the precursor. The ratio of PVA and PVA-MA was adjusted between 0:10 to 7:3 for achieving different properties.

Printer Setup. The homemade printer consists of an DLP-based PRO4500 UV light (385 nm) projector from Wintech Digital System Technology Corporation, a motorized translation stage mounted to a motor controller, and other optical accessories from Thorlabs, Inc. The power density of the projected UV light on the focal plane is measured to be 2.34 mW/cm^2 using an ultraviolet light meter, Traceable Products. A customized program was used to coordinate the projection of image and the movement of the stage. The resolution of the printer was 30 μm in the $x-y$ plane and 10 μm in the z-axis direction.

Printing Process. All the printing proceeded in air under ambient conditions. A 3D computer-aided design (CAD) models was first designed and sliced into series of 2D patterns. The patterns were sequentially projected onto the substrate, which was immersed in the precursor solution. The thickness of each layer was set to be 0.1 mm. Each layer was cured for 30 s. For printing the bilayer structures, a bottom layer was printed, rinsed with DI water to remove the unreacted precursor and dried. The printed layer was then immersed in a second precursor and a layer with different material was printed on the top. All the samples tested for following measurements of mechanical properties, contraction force, and swelling ratio were all printed by this process.

Salting-out Treatment. The printed hydrogels were first immersed in DI water for 24 h to remove the excess monomers and then immersed in 0.1−1 M Na_2SO_4 solution for 5 h to induce aggregation and crystallization of the PVA and PVA-MA chains.

Mechanical Properties Measurement. A Cellscale Univert mechanical tester was used for measuring passive mechanical properties and active contraction of the hydrogel. For passive tensile tests, dog bone specimens with 2 mm gauge width, 4 mm gauge length, and 2 mm thickness was 3D printed and measured using a 4.5 N loading cell under stretch rate of 0.1/s. For passive compression tests, cylindrical specimen with 5 mm diameter and 2 mm height was 3D printed and measured using a 10 N loading cell under compression rate of 0.01/s.

Contraction Force Measurement. For active contraction force measurement, the dog bone specimen was clamped at a fixed distance of 4 mm using the tensile testing setup with a water bath compartment installed; hot water was poured into the bath container and the contraction force was recorded using a 0.5 N loading cell.

Swelling Ratio Measurement. The cylindrical specimen for compression test was equilibrated in water and heated to 40 °C using a hot plate. The area change of the specimen was recorded using a camera from top. It is assumed that the specimen showed uniform volume change in all directions. The volumetric swelling ratio was calculated using the following:

$$\text{contraction ratio} = \left(\frac{\text{Area}_{40^\circ\text{C}}}{\text{Area}_{25^\circ\text{C}}}\right)^{3/2}$$

Microstructure Characterization. All hydrogel samples were immersed in DI water for 24 h before freeze-drying using a Labconco FreeZone freeze-dryer. The freeze-dried hydrogels were cut to expose the inside and sputtered with gold before carrying out imaging using a ZEISS Supra 40VP SEM.

XRD Characterization. The hydrogel sample was cut into a rectangular shape with dimensions of 2 cm × 1 cm x 4 mm and placed in rectangular sample holders for examination, and the resulting spectrum were analyzed by built-in database on Panalytical X'Pert Pro Powder X-ray Diffractometer.

DSC Characterization. Before freeze-drying the hydrogels for DSC measurements, we first used excess chemical cross-links induced

https://dx.doi.org/10.1021/acsami.0c17532
ACS Appl. Mater. Interfaces XXXX, XXX, XXX−XXX

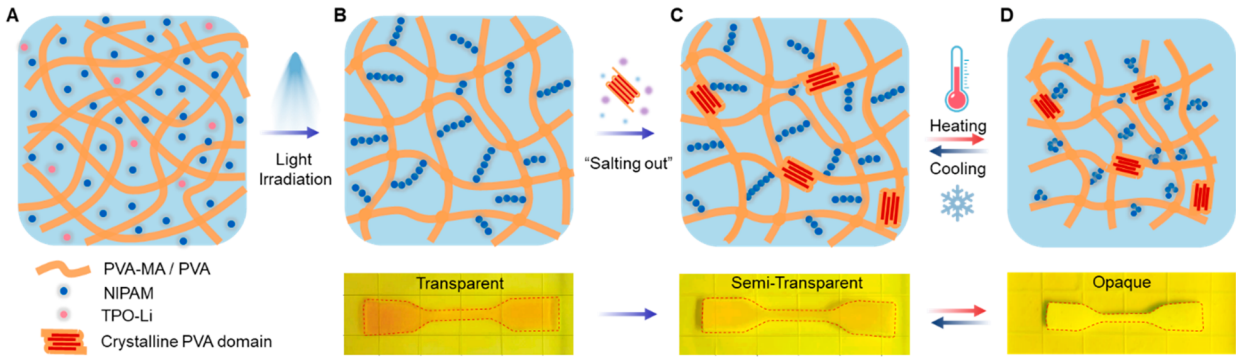

Figure 1. Illustration of the synthesis of PVA/(PVA-MA)-*g*-PNIPAM hydrogel. (A) Aqueous precursor containing PVA, PVA-MA, NIPAM and TPO-Li. (B) One-pot synthesis of PVA/(PVA-MA)-*g*-PNIPAM hydrogel by light irradiation from a DLP 3D printer. The as-printed hydrogel was transparent. (C) Toughening of hydrogel by immersion in Na_2SO_4 salt solution to induce PVA aggregation and crystallization. The hydrogel turned semitransparent after the salting-out process. (D) Actuation of the hydrogel by heating, and the recovery of hydrogel by cooling. The hydrogel turned completely opaque after heating and reverted to semitransparent after cooling.

by glutaraldehyde to fix the amorphous PVA polymer chains to minimize the further formation of crystalline domains during the freeze-drying process following ref 40. The water content of the hydrogel f_{water} could be obtained by comparing the weight before and after freeze-drying. In a typical DSC measurement, we first weighed the total mass of the freeze-dried sample, m. The sample was then placed in a Tzero pan and heated up from 40 to 250 °C at a rate of 20 °C/min under a nitrogen atmosphere. The curve of heat flow shows a narrow peak ranging from 200 to 250 °C, which corresponds to the melting of the crystalline domains. The integration of the endothermic curve from 200 to 250 °C gives the enthalpy for melting the crystalline domains per unit mass of the dry sample. The mass of the crystalline domains $m_{crystalline}$ can be calculated as $m_{crystalline} = mH_{crystalline}/H^0_{crystalline}$, in which $H^0_{crystalline}$ = 138.6 J/g is the enthalpy of fusion of 100 wt % crystalline PVA.[43] Therefore, the crystallinity in the dry sample X_{dry} can be calculated as $X_{dry} = m_{crystalline}/m$. With measured water content from freeze-drying, the crystallinity in the swollen state can be calculated as $X_{swollen} = X_{dry}(1 - f_{water})$.

FT-IR Characterization. The Fourier-transform infrared spectroscopy (FT-IR) analysis was conducted using a JASCO model 420 FT-IR using a potassium bromide (KBr) pellet. FT-IR spectra were recorded in the spectral range of 4000−400 cm^{-1} with a 2 cm^{-1} resolution and 32 scans.

RESULTS AND DISCUSSION

Material Design. Figure 1A, B showed the one-pot synthesis of the PVA/(PVA-MA)-*g*-PNIPAM hydrogel. PVA and PVA-MA were used as the tough polymer backbone for two reasons. First, because of the high molecular weight of PVA, the fracture energy of PVA chains are much higher than the relatively short polymer chains formed via radical polymerization from monomers. The energy required to fracture a polymer chain (Γ) scales proportionally with the polymer chains length (n repeating units) according to Lake−Thomas theory ($\Gamma \propto \sqrt{n}$).[39] Second, PVA is easy to crystallize via thermal annealing or phase separation processes.[40,41,44] The crystalline domains can toughen hydrogels by inhibiting crack propagation, cross-linking multiple chains, and increasing the fracture energy of polymer chains, as the energy required to fracture crystallized chains are much higher than that of its amorphous counterpart. For subsequent grafting of thermally responsive monomers onto the PVA chains, the PVA polymers went through a simple condensation reaction with methacrylic acid (MA) in an acidic environment and produced a UV cross-link-able derivative PVA polymer (Figure S2) with the hydroxyl (−OH) side groups partially modified with the methacrylate (-MA) side groups, termed as PVA-MA (Figure S1A). However, note that PVA-MA has reduced ability to crystallize due to the steric hindrance by the modified side group. Therefore, nonmodified pristine PVA was blended with PVA-MA in the precursor for retaining good crystallization ability for toughening the hydrogel. Additionally, PVA-MA is crucial for the grating of NIPAM molecules onto the PVA network, which in turn gave rise to the thermal responsiveness of the hydrogel. Therefore, a balanced concentration of PVA and PVA-MA should be used for optimum combined mechanical properties and thermal responsiveness. The hydrogels were denoted as "*x*P-MA_(10-*x*)P" for *x* wt % of PVA-MA added in the total precursor, and we mainly used 5P-MA_5P hydrogel in our study due to its combined high strength, high stretchability and good thermal responsiveness. Additionally, water was used as the solvent instead of organic solvents for green synthesis, and TPO-Li was used as the photoinitiator in the aqueous precursor, due to its ability to induce radical polymerization under both visible and UV spectra to fit different printing systems. PVA, PVA-MA, NIPAM, and TPO-Li were dissolved in water (Figure 1A) and exposed to UV light for gelation (Figure 1B). No cross-linker was added to ensure that all retained NIPAM molecules were attached to the PVA-MA backbone after rinsing. The fabricated hydrogel was transparent and colored with the photo absorber dye added to the precursor (Figure 1B, bottom image). The chemical composition of the obtained hydrogel was verified with FT-IR analysis (Figure S1B).

To further toughen the PVA/(PVA-MA)-*g*-PNIPAM hydrogel, the 3D printed sample was then immersed into Na_2SO_4 salt solutions of various concentrations to induce aggregation and crystallization of the PVA chains. The treatment is known as salting out and is based on the classical Hofmeister effect, in which different ions have a distinguishable ability to induce phase separation of solutes and precipitate the dissolved polymers.[45] The sulfate ions have a strong ability to induce aggregation and crystallization of the PVA and were used as the salting-out agent in this study.[20,44,46] The sample transitioned from transparent to semitransparent after the salting-out treatment and remained semitransparent even when immersed back into water, indicating the formation of nanocrystalline domains that strongly scattered light (Figure 1C, Figure S3).

https://dx.doi.org/10.1021/acsami.0c17532
ACS Appl. Mater. Interfaces XXXX, XXX, XXX−XXX

The toughened PVA/(PVA-MA)-*g*-PNIPAM hydrogel by salting out maintained the reversible thermal responsiveness in water (Figure 1D), benefiting from the single network design. The thermal-responsive side groups/side chains were combined with the tough hydrogel network, which reduced the internal constraint between the thermal responsive and non-thermal responsive domains in the hydrogel network. When heated above the LCST of PNIPAM, the hydrogel quickly turned opaque as the grafted NIPAM chains phase separated from water and formed globules that additionally scattered light. The volume change was slower than the color change because of the hydrogel's bulk size, and the hydrogel gradually shrunk in size over time. This could be caused by the relatively small pore size (0.2−2 μm) and bulk sample size of the hydrogel, which hindered the diffusion of water in/out of the hydrogel network (Figure S4). When lowering the bath temperature to below LCST, the hydrogel could recover to the original size and color. Because of the 3D printability of the hydrogel, large voids serving as efficient water channels could be printed in the hydrogel structure for bypassing the size-dependent volume change of the hydrogel and increase actuation speed.

Passive Mechanical Properties. The typical tensile and compressive stress−strain curves of the printed PVA/(PVA-MA)-*g*-PNIPAM hydrogel with respect to concentration of Na_2SO_4 solution are shown in Figure 2A, B. All hydrogels were

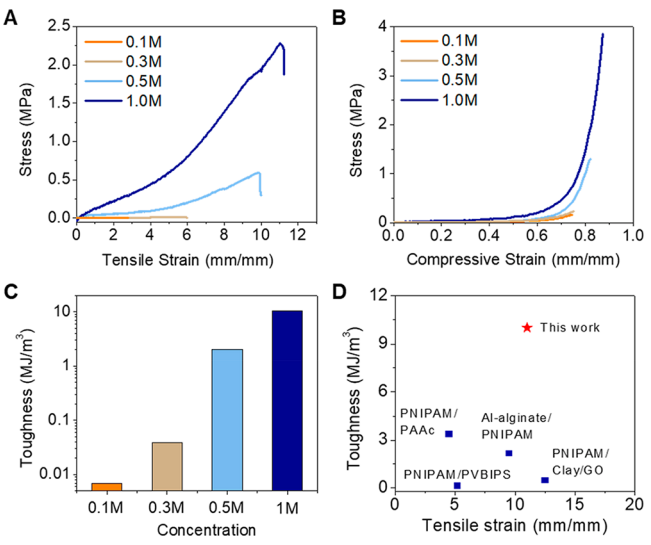

Figure 2. Mechanical properties of PVA/(PVA-MA)-*g*-PNIPAM hydrogels. (A, B) Tensile and compressive stress−strain curves of 5P-MA_5P hydrogel toughened in different concentrations of Na_2SO_4 salt solution. (C) Tensile toughness of 5P-MA_5P hydrogels that were toughened in different concentrations of Na_2SO_4 salt solutions. (D) Ashby diagram showing the toughness vs strain properties of 5P-MA_5P hydrogel compared with other tough NIPAM hydrogel systems.

rinsed in DI water to remove the salt prior to mechanical testing. The maximum stress and strain of the hydrogel increased with the concentration of Na_2SO_4 used for salting out, mainly due to the increasing aggregation and crystallinity of the hydrogel with increasing concentration of salting out agent (Figure 2A, B, Figure S5). The typical 5P-MA_5P hydrogel reached ∼15% crystallinity against the total solid content corresponding to ∼1.5% crystallinity in the wet state after salting out for 5 h. The PVA crystalline domains significantly strengthened the hydrogel by their ability to pin down cracks,[41] they also improved hydrogel's elasticity by acting as rigid high functionality cross-linkers.[13]

For a typical 5P-MA_5P hydrogel, the tensile strength increased from 0.015 to 2.2 MPa (Figure 2A), and the compressive strength increased from 0.16 to 3.8 MPa (Figure 2B) after the salting-out treatment in 1 M Na_2SO_4 solution. The corresponding toughness of the 5P-MA_5P hydrogel reached 10 MJ/m^3 (Figure 2C), comparable to that of natural tendons. Compared with other double-network tough NIPAM hydrogels,[30,47−49] the PVA/(PVA-MA)-*g*-PNIPAM hydrogel showed high stretchability, strength, and toughness (Figure 2D).

Active Actuation Properties. The PVA/(PVA-MA)-*g*-PNIPAM hydrogel maintained thermal responsiveness after the toughening process by salting out (Figure 3A−C),

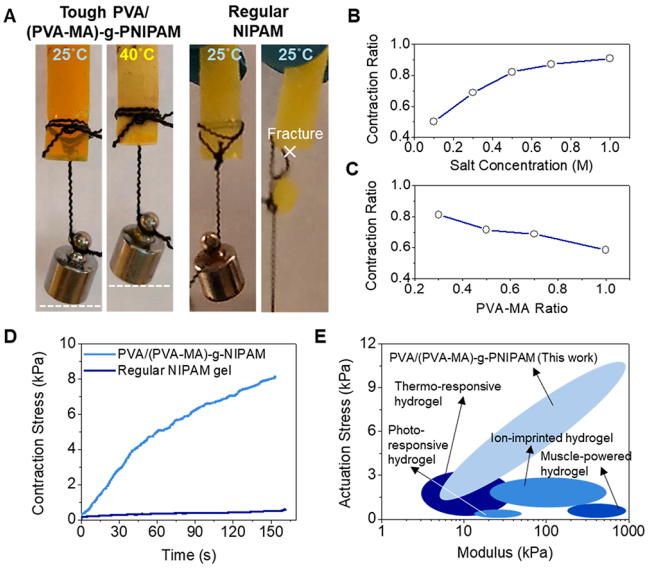

Figure 3. Actuation and output stress of PVA/(PVA-MA)-*g*-PNIPAM hydrogel. (A) Application of PVA/(PVA-MA)-*g*-PNIPAM hydrogel as linear actuator compared with NIPAM hydrogel. The 5P-MA_5P hydrogel toughened in 0.5 M Na_2SO_4 solution could lift a 20 g weight without fracture while regular NIPAM hydrogel of the same dimension fractured easily. (B) Contraction ratio of the 5P-MA_5P hydrogel toughened in different concentrations of Na_2SO_4 solution. (C) Contraction ratio of PVA/(PVA-MA)-*g*-PNIPAM hydrogel with different PVA to PVA-MA ratio toughened in 0.3 M Na_2SO_4 solution. (D) Stress−time curve of 5P-MA_5P hydrogel toughened in 0.5 M Na_2SO_4 solution compared with regular PNIPAM hydrogel. (E) Ashby diagram showing the actuation stress vs modulus of the PVA/(PVA-MA)-*g*-PNIPAM hydrogel compared with other hydrogel actuators.

benefiting from the combination of thermal responsive side groups and tough polymer main chains in a single network. For a typical 5P-MA_5P hydrogel, the volumetric contraction could reach 50% for hydrogels toughened in 0.1 M Na_2SO_4, comparable to the pure PNIPAM hydrogel (60% contraction). Although the volumetric contraction decreased with increasing salt concentration, which was due to the reduced polymer chain mobility as the PVA and (PVA-MA)-*g*-PNIPAM polymer chains aggregated and crystallized during the salting-out process, the ultratough 5P-MA_5P hydrogel toughened in 1 M Na_2SO_4 still maintained around 10% volumetric contraction (Figure 3B). The PVA/PVA-MA ratio also showed

https://dx.doi.org/10.1021/acsami.0c17532
ACS Appl. Mater. Interfaces XXXX, XXX, XXX−XXX

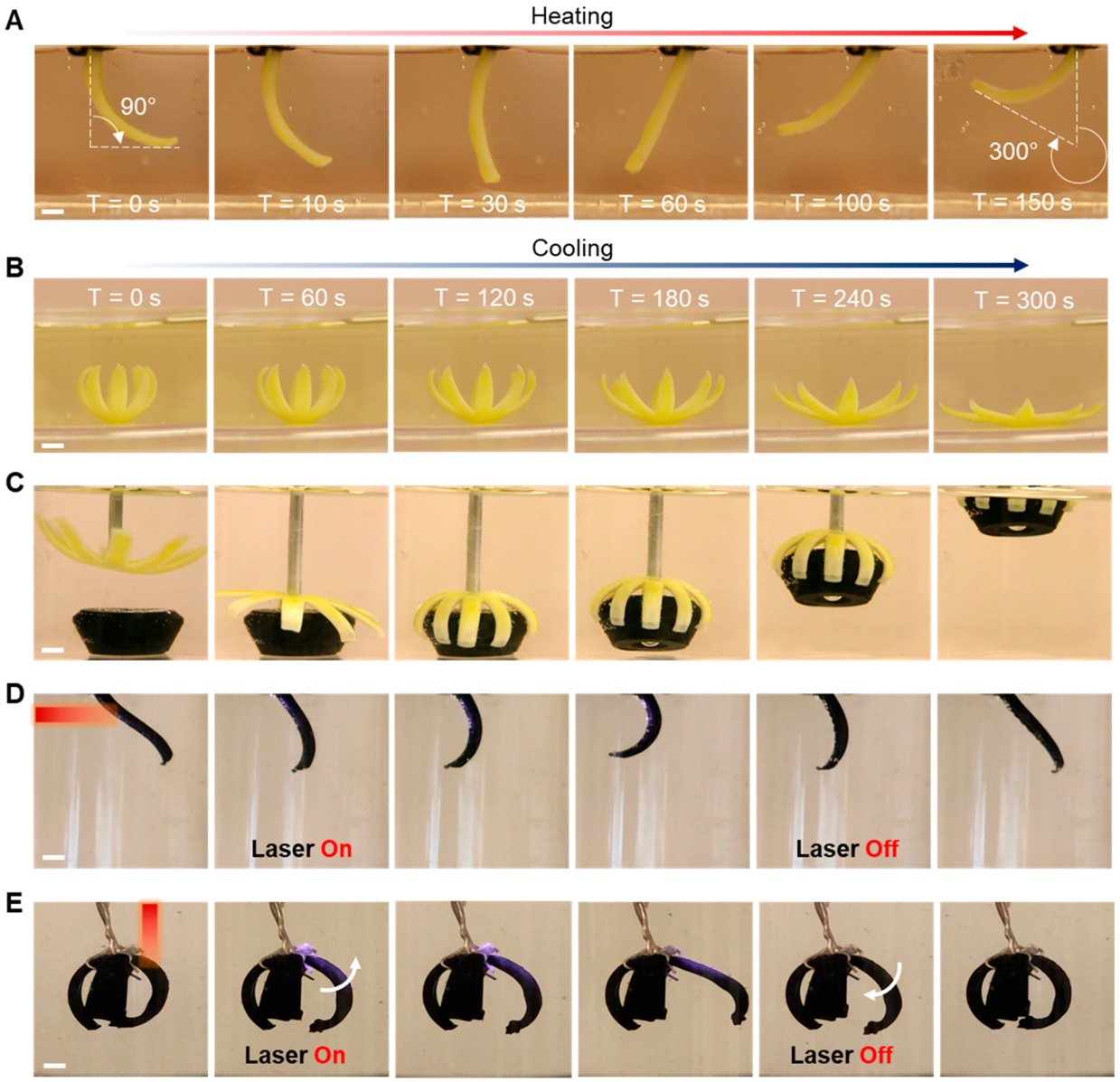

Figure 4. Customized actuator geometry and actuation speed. (A) Printed bilayer beam actuator showing fast bending and large bending angle under heating. (B) Bilayer flower blooms under cooling. (C) 3D printed bilayer gripper picking up an object through thermal actuation. The object weighs 1 g. (D) Remote actuation of bilayer beam actuator coated with a thin layer of poly(pyrrole). (E) Remote and selective actuation of bilayer gripper actuator coated with a thin layer of poly(pyrrole). Scale bar: 1 mm.

effect on the swelling ratio (Figure 3C). The contraction of the PVA/(PVA-MA)-*g*-PNIPAM hydrogel increased with the PVA-MA concentration. On one hand, higher PVA content increased the aggregates and crystalline domains formed during salting out for better toughening of the hydrogel (Figure S6A−C) but provided fewer grafting sites for increasing thermal responsiveness of the hydrogel network. On the other hand, higher PVA-MA increased the amount of NIPAM grafted to the hydrogel network, which in turn improved the thermal responsiveness of the hydrogel, but would lead to higher chemical cross-linking density[50,51] (Figure S7), which reduced the maximum strain of the hydrogel (Figure S6A−C).

With the combined high toughness and thermal responsiveness, a typical 5P-MA_5P hydrogel strip fabricated via 4D printing and subsequently toughened in 0.5 M Na_2SO_4 could lift heavy weights (20 g) without large passive deformation or fracture (Figure 3A, left). In contrast, a conventional NIPAM hydrogel (fabricated by polymerizing 30 wt % NIPAM, 1.5 wt % Bis, and 1 wt % Irgacure 2959 in DMSO and immersed back into DI water) with the same dimensions deformed severely under the same weight, which leads to the formation and propagation of cracks in the hydrogel and eventually fracture of the hydrogel (Figure 3A, right). We quantitatively measured the contraction force delivered by the two hydrogels, and the tough 5P-MA_5P hydrogel showed ∼20 times higher contraction force than the conventional NIPAM hydrogel (Figure 3D). Compared to various state-of-the-art hydrogel actuators,[52−56] the tough PVA/(PVA-MA)-*g*-PNIPAM hydrogel showed a relatively high actuation force and modulus (Figure 3E).

The deliverable force of the PVA/(PVA-MA)-*g*-PNIPAM hydrogel is positively related with the mechanical properties of the hydrogel (Figure 3E). Without toughening by salting out,

https://dx.doi.org/10.1021/acsami.0c17532
ACS Appl. Mater. Interfaces XXXX, XXX, XXX−XXX

the contraction force of the PVA/(PVA-MA)-*g*-PNIPAM hydrogel is comparable to that of the conventional NIPAM hydrogel. With increasing toughness of the PVA/(PVA-MA)-*g*-PNIPAM hydrogel by using higher concentration salt solution, the contraction force also increased. The reason for this relationship is as follows: The nontoughened PVA/(PVA-MA)-*g*-PNIPAM is intrinsically soft, which would deform severely under low stress. While the hydrogel could contract significantly upon heating when there is no external load, the displacement is reduced when external load exists due to the passive extension of the hydrogel under stress. Thus, the tension between hydrogel and object is relaxed due to this passive deformation which reduced the force being delivered externally (Figure S8A). Additionally, in the case of high external loading, the hydrogel would immediately fracture due to its low strength and toughness. On the contrary, the toughened PVA/(PVA-MA)-*g*-PNIPAM hydrogel has a much higher modulus and would show reduced passive deformation under external loading. The toughened hydrogel could also endure much higher external force. Thus, the tension between the toughened hydrogel and the external object was maintained at a much higher value and the toughened hydrogel contracted without large passive extension under tension, which led to the increased deliverable force (Figure S8B).

Demonstration of Thermal/Photo Actuators with High Force and Fast Actuation. With high toughness and actuation force, the PVA/(PVA-MA)-*g*-PNIPAM hydrogels could readily be applied to fabricate hydrogel actuators. By 4D printing, bilayer actuators of various geometry could be facilely fabricated. The bilayer actuators consist of a passive layer of PVA/PVA-MA hydrogel and an active layer of PVA/(PVA-MA)-*g*-PNIPAM hydrogel (Figure S9). The printed bilayer actuators were washed in DI water and immersed in 0.5 M Na_2SO_4 salt for toughening. After toughening, the bilayer actuators were immersed back in water for actuation tests. Figure 4A showed the actuation of a bilayer beam by heating. The bilayer beam was initially bent toward the passive layer because of the higher shrinkage of PVA/PVA-MA hydrogel compared to PVA/(PVA-MA)-*g*-PNIPAM hydrogel. Upon heating, the bilayer beam quickly bent toward the active layer. Despite the initial reverse bending, the bilayer beam completely bent toward the passive layer within 150 s and showed a large bending angle of ~210° at the tip (Movie S1). Figure 4B showed the actuation of a bilayer flower by cooling. The flower petals were initially bent by heating. When immersed in a room-temperature water bath, the active layer gradually expanded, which led to the blooming of the bilayer flower (Movie S2). By spatially programming the area ratio of the passive/active layer (Figure S9B), the flower petals after blooming did not overbend toward the passive layer. Combining high strength, high toughness, high actuation force, and 4D printing aided design, a thermally activated bilayer tough hydrogel gripper was demonstrated (Figure 4C). Upon heating, the gripper arm bent toward the object and locked onto the object, which enabled the subsequent lifting of the object out of the water bath. In contrast, while a conventional NIPAM hydrogel gripper of the same geometry showed good actuation performance, it deformed severely during the lifting process and failed to lift the same object (Movie S3). Note that the arms of the PVA/(PVA-MA)-*g*-PNIPAM hydrogel gripper did not show a large deformation during the lifting process, because of the high strength and contraction force of the hydrogel. The weight being lifted weighed 1 g, which is approximately 5 times the weight of the solid content of the hydrogel gripper.

Remote activatability is a significant advantage of NIPAM-based hydrogels due to the facile conversion of photons to thermal energy through various photoabsorbers.[4,6] The photoabsorbers are generally black materials with nanometer sizes for maximum photothermal conversion efficiency; here, we utilized poly(pyrrole) as the photoabsorber coating. As shown in Figure 4D, E, the bilayer hydrogel actuator turned black after coating with poly(pyrrole) and gained remote activatability using an IR laser (50 mW). The illuminated part on the hydrogel actuators was locally heated quickly to induce bending, whereas the unilluminated parts remained cool and static (Movies S4 and S5). By controlling the illumination, good spatial control of actuation could be realized in the hydrogel actuator (Figure 4E).

Actuation speed is another important criterion of the hydrogel actuator. Because of the diffusion-mediated swelling and contraction of hydrogels, the actuation speed inversely scales with the actuator size. Utilizing the ability to spatially program the hydrogel, the size-dependent actuation speed of PVA/(PVA-MA)-*g*-PNIPAM hydrogels could be bypassed by printing large voids into the hydrogel to facilitate the fast diffusion of water in and out of the hydrogel. Figure 5A showed three types of printed 5P-MA_5P hydrogel lattice, respectively, with Kelvin cell, simple cubic, and octet truss unit cells. These hydrogel lattices were originally weak and collapsed in air in the as-printed state (Figure S10A); after toughening in 0.5 M Na_2SO_4, they became capable of self-supporting their own weight and retaining the designed structure in air as a stand-alone architecture (Figure S10B). When using the lattice design with octet truss cells, the lattice could tolerate high external loading and deformation and still recover (Figure 5B). Applying the lattice design in printing hydrogel structures, the latticed 5P-MA_5P hydrogel toughened in 0.5 M Na_2SO_4 showed a 4 times faster contraction speed compared to a nonstructured bulk PVA/(PVA-MA)-*g*-PNIPAM hydrogel (Figure 5C, D). The latticed hydrogel also showed an increased contraction ratio compared to its nonstructured counterpart (Movie S6). Therefore, with structural design and the aid of 4D printing, a fast actuation

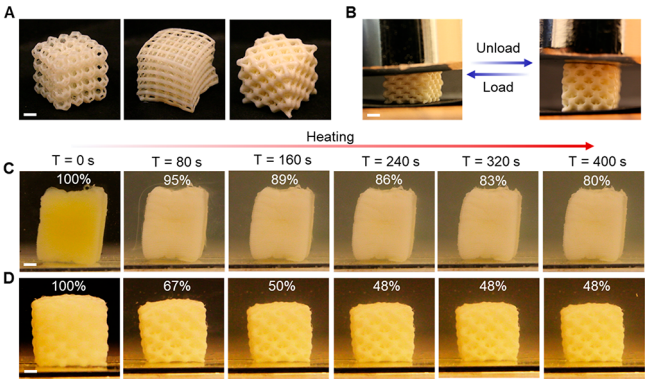

Figure 5. (A, B) Lattice structured 5P-MA_5P hydrogels toughened in 0.5 M Na_2SO_4 showing self-support in air and recoverability after deformed. (C, D) Boosting the actuation speed and contraction ratio by printing lattice structured hydrogel in comparison with a bulk hydrogel of the same bulk volume. Scale bar: 2 mm.

https://dx.doi.org/10.1021/acsami.0c17532
ACS Appl. Mater. Interfaces XXXX, XXX, XXX−XXX

speed could be achieved in addition to the previously demonstrated high toughness and contraction force.

CONCLUSION

In summary, we have demonstrated a material design that consists of stimuli-responsive monomers and tough polymers in a single hydrogel network for combined high toughness and high actuation performance. Specifically, we showcased this design by grafting thermal-responsive NIPAM monomers to tough PVA/PVA-MA hydrogel network in a one-pot synthesis. We have evaluated the effect of salt concentration, PVA/PVA-MA ratio, and structural design on the mechanical and actuation performance of the PVA/(PVA-MA)-*g*-PNIPAM hydrogel. Utilizing the combined high toughness and improved actuation force of the PVA/(PVA-MA)-*g*-PNIPAM hydrogels, bilayer actuators were fabricated via 4D printing for demonstration. Remote actuation using light was also demonstrated using a photothermal energy conversion route. Overall, the presented material design significantly improved material toughness while maintaining high swelling/contraction of the hydrogel. We are convinced that the presented design would benefit the fabrication of hydrogel actuators and robotics for practical applications and would lay the path for new pH-responsive, magnetoresponsive, humidity-responsive hydrogel systems with both high toughness and high actuation performances.

ASSOCIATED CONTENT

Supporting Information

The following files are available free of charge. The Supporting Information is available free of charge at https://pubs.acs.org/doi/10.1021/acsami.0c17532.

Figures S1−S10 (PDF)

Movie S1: Thermal-induced bending of a bilayer beam (MP4)

Movie S2: Thermal-induced blooming of a bilayer flower (MP4)

Movie S3: Comparison of tough and conventional hydrogel grippers (MP4)

Movie S4: Light-induced bending of a bilayer beam (MP4)

Movie S5: Light-induced actuation of a bilayer gripper (MP4)

Movie S6: Comparison of bulk hydrogel and lattice structured hydrogel (MP4)

AUTHOR INFORMATION

Corresponding Author

Ximin He − *Department of Materials Science and Engineering, University of California Los Angeles, Los Angeles, California 90095, United States;* orcid.org/0000-0001-8845-4637; Email: ximinhe@ucla.edu

Authors

Mutian Hua − *Department of Materials Science and Engineering, University of California Los Angeles, Los Angeles, California 90095, United States*

Dong Wu − *Department of Materials Science and Engineering, University of California Los Angeles, Los Angeles, California 90095, United States*

Shuwang Wu − *Department of Materials Science and Engineering, University of California Los Angeles, Los Angeles, California 90095, United States*

Yanfei Ma − *Department of Materials Science and Engineering, University of California Los Angeles, Los Angeles, California 90095, United States; State Key Laboratory of Solid Lubrication, Lanzhou Institute of Chemical Physics, Chinese Academy of Sciences, Lanzhou 730000, China*

Yousif Alsaid − *Department of Materials Science and Engineering, University of California Los Angeles, Los Angeles, California 90095, United States*

Complete contact information is available at: https://pubs.acs.org/10.1021/acsami.0c17532

Author Contributions

†M.H. and D.W. contributed equally to this work. X.H. and M.H. proposed the idea and X.H. supervised the research. M.H. and D.W. designed and performed the experiments. M.H. analyzed the data. M.H., D.W., and X.H. wrote the manuscript. All authors discussed the manuscript.

Notes

The authors declare no competing financial interest.

ACKNOWLEDGMENTS

The authors acknowledge the support of ONR award N000141712117, ONR award N00014-18-1-2314, AFOSR award FA9550-17-1-0311, AFOSR award FA9550-18-1-0449, AFOSR award FA9550-20-1-0344, NSF CAREER award 1724526, the Hellman Fellows Funds, and start-up funds from the University of California, Los Angeles

REFERENCES

(1) Ionov, L. Hydrogel-Based Actuators: Possibilities and Limitations. *Mater. Today* **2014**, *17* (10), 494−503.

(2) Yuk, H.; Varela, C. E.; Nabzdyk, C. S.; Mao, X.; Padera, R. F.; Roche, E. T.; Zhao, X. Dry Double-Sided Tape for Adhesion of Wet Tissues and Devices. *Nature* **2019**, *575* (7781), 169−174.

(3) Liu, X.; Liu, J.; Lin, S.; Zhao, X. Hydrogel Machines. *Mater. Today* **2020**, *36*, 102−124.

(4) Zhao, Y.; Xuan, C.; Qian, X.; Alsaid, Y.; Hua, M.; Jin, L.; He, X. Soft Phototactic Swimmer Based on Self-Sustained Hydrogel Oscillator. *Sci. Robot.* **2019**, *4* (33), eaax7112.

(5) Yuk, H.; Lin, S.; Ma, C.; Takaffoli, M.; Fang, N. X.; Zhao, X. Hydraulic Hydrogel Actuators and Robots Optically and Sonically Camouflaged in Water. *Nat. Commun.* **2017**, *8* (1), 14230.

(6) Qian, X.; Zhao, Y.; Alsaid, Y.; Wang, X.; Hua, M.; Galy, T.; Gopalakrishna, H.; Yang, Y.; Cui, J.; Liu, N.; Marszewski, M.; Pilon, L.; Jiang, H.; He, X. Artificial Phototropism for Omnidirectional Tracking and Harvesting of Light. *Nat. Nanotechnol.* **2019**, *14* (11), 1048−1055.

(7) Xu, X.; Liu, Y.; Fu, W.; Yao, M.; Ding, Z.; Xuan, J.; Li, D.; Wang, S.; Xia, Y.; Cao, M. Poly(N-Isopropylacrylamide)-Based Thermoresponsive Composite Hydrogels for Biomedical Applications. *Polymers (Basel)* **2020**, *12* (3), 580.

(8) D'Eramo, L.; Chollet, B.; Leman, M.; Martwong, E.; Li, M.; Geisler, H.; Dupire, J.; Kerdraon, M.; Vergne, C.; Monti, F.; Tran, Y.; Tabeling, P. Microfluidic Actuators Based on Temperature-Responsive Hydrogels. *Microsystems Nanoeng.* **2018**, *4* (1), 17069.

(9) Tang, L.; Wang, L.; Yang, X.; Feng, Y.; Li, Y.; Feng, W. Poly(N-Isopropylacrylamide)-Based Smart Hydrogels: Design, Properties and Applications. *Prog. Mater. Sci.* **2021**, *115*, 100702.

(10) Guo, J.; Yang, W.; Deng, Y.; Wang, C.; Fu, S. Organic-Dye-Coupled Magnetic Nanoparticles Encaged inside Thermoresponsive PNIPAM Microcapsules. *Small* **2005**, *1* (7), 737−743.

(11) Hu, X.; Vatankhah-Varnoosfaderani, M.; Zhou, J.; Li, Q.; Sheiko, S. S. Weak Hydrogen Bonding Enables Hard, Strong, Tough, and Elastic Hydrogels. *Adv. Mater.* **2015**, *27* (43), 6899−6905.
(12) Sun, J. Y.; Zhao, X.; Illeperuma, W. R. K.; Chaudhuri, O.; Oh, K. H.; Mooney, D. J.; Vlassak, J. J.; Suo, Z. Highly Stretchable and Tough Hydrogels. *Nature* **2012**, *489* (7414), 133−136.
(13) Zhao, X. Multi-Scale Multi-Mechanism Design of Tough Hydrogels: Building Dissipation into Stretchy Networks. *Soft Matter* **2014**, *10* (5), 672−687.
(14) Shibayama, M. Structure-Mechanical Property Relationship of Tough Hydrogels. *Soft Matter* **2012**, *8* (31), 8030−8038.
(15) Haq, M. A.; Su, Y.; Wang, D. Mechanical Properties of PNIPAM Based Hydrogels: A Review. *Mater. Sci. Eng., C* **2017**, *70*, 842−855.
(16) Illeperuma, W. R. K.; Sun, J. Y.; Suo, Z.; Vlassak, J. J. Force and Stroke of a Hydrogel Actuator. *Soft Matter* **2013**, *9* (35), 8504−8511.
(17) Depa, K.; Strachota, A.; Šlouf, M.; Hromádková, J. Fast Temperature-Responsive Nanocomposite PNIPAM Hydrogels with Controlled Pore Wall Thickness: Force and Rate of T-Response. *Eur. Polym. J.* **2012**, *48* (12), 1997−2007.
(18) Gong, J. P.; Katsuyama, Y.; Kurokawa, T.; Osada, Y. Double-Network Hydrogels with Extremely High Mechanical Strength. *Adv. Mater.* **2003**, *15* (14), 1155−1158.
(19) Lin, P.; Ma, S.; Wang, X.; Zhou, F. Molecularly Engineered Dual-Crosslinked Hydrogel with Ultrahigh Mechanical Strength, Toughness, and Good Self-Recovery. *Adv. Mater.* **2015**, *27* (12), 2054−2059.
(20) Yang, Y.; Wang, X.; Yang, F.; Shen, H.; Wu, D. A Universal Soaking Strategy to Convert Composite Hydrogels into Extremely Tough and Rapidly Recoverable Double-Network Hydrogels. *Adv. Mater.* **2016**, *28* (33), 7178−7184.
(21) Takahashi, R.; Sun, T. L.; Saruwatari, Y.; Kurokawa, T.; King, D. R.; Gong, J. P. Creating Stiff, Tough, and Functional Hydrogel Composites with Low-Melting-Point Alloys. *Adv. Mater.* **2018**, *30* (16), 1706885.
(22) Lin, S.; Cao, C.; Wang, Q.; Gonzalez, M.; Dolbow, J. E.; Zhao, X. Design of Stiff, Tough and Stretchy Hydrogel Composites via Nanoscale Hybrid Crosslinking and Macroscale Fiber Reinforcement. *Soft Matter* **2014**, *10* (38), 7519−7527.
(23) Huang, Y.; King, D. R.; Sun, T. L.; Nonoyama, T.; Kurokawa, T.; Nakajima, T.; Gong, J. P. Energy-Dissipative Matrices Enable Synergistic Toughening in Fiber Reinforced Soft Composites. *Adv. Funct. Mater.* **2017**, *27* (9), 1605350.
(24) Xiang, C.; Wang, Z.; Yang, C.; Yao, X.; Wang, Y.; Suo, Z. Stretchable and Fatigue-Resistant Materials. *Mater. Today* **2020**, *34*, 7−16.
(25) Illeperuma, W. R. K.; Sun, J. Y.; Suo, Z.; Vlassak, J. J. Fiber-Reinforced Tough Hydrogels. *Extrem. Mech. Lett.* **2014**, *1*, 90−96.
(26) Tian, Y.; Wei, X.; Wang, Z. J.; Pan, P.; Li, F.; Ling, D.; Wu, Z. L.; Zheng, Q. A Facile Approach to Prepare Tough and Responsive Ultrathin Physical Hydrogel Films as Artificial Muscles. *ACS Appl. Mater. Interfaces* **2017**, *9* (39), 34349−34355.
(27) Zheng, S. Y.; Shen, Y.; Zhu, F.; Yin, J.; Qian, J.; Fu, J.; Wu, Z. L.; Zheng, Q. Programmed Deformations of 3D-Printed Tough Physical Hydrogels with High Response Speed and Large Output Force. *Adv. Funct. Mater.* **2018**, *28* (37), 1803366.
(28) Peng, X.; Li, Y.; Zhang, Q.; Shang, C.; Bai, Q. W.; Wang, H. Tough Hydrogels with Programmable and Complex Shape Deformations by Ion Dip-Dyeing and Transfer Printing. *Adv. Funct. Mater.* **2016**, *26* (25), 4491−4500.
(29) Liu, X.; He, B.; Wang, Z.; Tang, H.; Su, T.; Wang, Q. Tough Nanocomposite Ionogel-Based Actuator Exhibits Robust Performance. *Sci. Rep.* **2015**, *4*, 1−7.
(30) Xiao, S.; Zhang, M.; He, X.; Huang, L.; Zhang, Y.; Ren, B.; Zhong, M.; Chang, Y.; Yang, J.; Zheng, J. Dual Salt- and Thermoresponsive Programmable Bilayer Hydrogel Actuators with Pseudo-Interpenetrating Double-Network Structures. *ACS Appl. Mater. Interfaces* **2018**, *10* (25), 21642−21653.
(31) Baker, A. B.; Wass, D. F.; Trask, R. S. Thermally Induced Reversible and Reprogrammable Actuation of Tough Hydrogels Utilising Ionoprinting and Iron Coordination Chemistry. *Sens. Actuators, B* **2018**, *254*, 519−525.
(32) Scherzinger, C.; Schwarz, A.; Bardow, A.; Leonhard, K.; Richtering, W. Cononsolvency of Poly-N-Isopropyl Acrylamide (PNIPAM): Microgels versus Linear Chains and Macrogels. *Curr. Opin. Colloid Interface Sci.* **2014**, *19* (2), 84−94.
(33) Zhang, Y.; Furyk, S.; Bergbreiter, D. E.; Cremer, P. S. Specific Ion Effects on the Water Solubility of Macromolecules: PNIPAM and the Hofmeister Series. *J. Am. Chem. Soc.* **2005**, *127* (41), 14505−14510.
(34) Yang, C.; Liu, Z.; Chen, C.; Shi, K.; Zhang, L.; Ju, X. J.; Wang, W.; Xie, R.; Chu, L. Y. Reduced Graphene Oxide-Containing Smart Hydrogels with Excellent Electro-Response and Mechanical Properties for Soft Actuators. *ACS Appl. Mater. Interfaces* **2017**, *9* (18), 15758−15767.
(35) Li, Y.; Sun, Y.; Xiao, Y.; Gao, G.; Liu, S.; Zhang, J.; Fu, J. Electric Field Actuation of Tough Electroactive Hydrogels Cross-Linked by Functional Triblock Copolymer Micelles. *ACS Appl. Mater. Interfaces* **2016**, *8* (39), 26326−26331.
(36) Gelebart, A. H.; Vantomme, G.; Meijer, E. W.; Broer, D. J. Mastering the Photothermal Effect in Liquid Crystal Networks: A General Approach for Self-Sustained Mechanical Oscillators. *Adv. Mater.* **2017**, *29* (18), 1606712.
(37) Jan Mulder, D.; Selinger, R. L. B.; Konya, A.; Gelebart, A. H.; Varga, M.; Vantomme, G.; Meijer, E. W.; Broer, D. J. Making Waves in a Photoactive Polymer Film. *Nature* **2017**, *546* (7660), 632−636.
(38) Ma, M.; Guo, L.; Anderson, D. G.; Langer, R. Bio-Inspired Polymer Composite Actuator and Generator Driven by Water Gradients. *Science (Washington, DC, U. S.)* **2013**, *339* (6116), 186−189.
(39) Lake, G. J.; Thomas, A. G. The Strength of Highly Elastic Materials. *Proc. R. Soc. London. Ser. A. Math. Phys. Sci.* **1967**, *300* (1460), 108−119.
(40) Lin, S.; Liu, J.; Liu, X.; Zhao, X. Muscle-like Fatigue-Resistant Hydrogels by Mechanical Training. *Proc. Natl. Acad. Sci. U. S. A.* **2019**, *116* (21), 10244−10249.
(41) Lin, S.; Liu, X.; Liu, J.; Yuk, H.; Loh, H.-C.; Parada, G. A.; Settens, C.; Song, J.; Masic, A.; McKinley, G. H.; Zhao, X. Anti-Fatigue-Fracture Hydrogels. *Sci. Adv.* **2019**, *5* (1), eaau8528.
(42) Wu, D.; Song, J.; Zhai, Z.; Hua, M.; Kim, C.; Frenkel, I.; Jiang, H.; He, X. Visualizing Morphogenesis through Instability Formation in 4-D Printing. *ACS Appl. Mater. Interfaces* **2019**, *11* (50), 47468−47475.
(43) Peppas, N. A.; Merrill, E. W. Differential Scanning Calorimetry of Crystallized PVA Hydrogels. *J. Appl. Polym. Sci.* **1976**, *20* (6), 1457−1465.
(44) Bai, R.; Yang, J.; Morelle, X. P.; Suo, Z. Flaw-Insensitive Hydrogels under Static and Cyclic Loads. *Macromol. Rapid Commun.* **2019**, *40* (8), 1800883.
(45) Kunz, W.; Henle, J.; Ninham, B. W. Zur Lehre von Der Wirkung Der Salze" (about the Science of the Effect of Salts): Franz Hofmeister's Historical Papers. *Curr. Opin. Colloid Interface Sci.* **2004**, *9* (1−2), 19−37.
(46) He, Q.; Huang, Y.; Wang, S. Hofmeister Effect-Assisted One Step Fabrication of Ductile and Strong Gelatin Hydrogels. *Adv. Funct. Mater.* **2018**, *28* (5), 1705069.
(47) Wang, T.; Huang, J.; Yang, Y.; Zhang, E.; Sun, W.; Tong, Z. Bioinspired Smart Actuator Based on Graphene Oxide-Polymer Hybrid Hydrogels. *ACS Appl. Mater. Interfaces* **2015**, *7* (42), 23423−23430.
(48) Zheng, W. J.; An, N.; Yang, J. H.; Zhou, J.; Chen, Y. M. Tough Al-Alginate/Poly(N -Isopropylacrylamide) Hydrogel with Tunable LCST for Soft Robotics. *ACS Appl. Mater. Interfaces* **2015**, *7* (3), 1758−1764.
(49) Wang, Y. J.; Li, C. Y.; Wang, Z. J.; Zhao, Y.; Chen, L.; Wu, Z. L.; Zheng, Q. Hydrogen Bond-Reinforced Double-Network Hydro-

https://dx.doi.org/10.1021/acsami.0c17532
ACS Appl. Mater. Interfaces XXXX, XXX, XXX−XXX

gels with Ultrahigh Elastic Modulus and Shape Memory Property. *J. Polym. Sci., Part B: Polym. Phys.* **2018**, *56* (19), 1281−1286.
(50) Jiang, H.; Su, W.; Mather, P. T.; Bunning, T. J. Rheology of Highly Swollen Chitosan/Polyacrylate Hydrogels. *Polymer* **1999**, *40* (16), 4593−4602.
(51) Flory, P. J. Molecular Theory of Rubber Elasticity. *Polym. J.* **1985**, *17* (1), 1−12.
(52) Cvetkovic, C.; Raman, R.; Chan, V.; Williams, B. J.; Tolish, M.; Bajaj, P.; Sakar, M. S.; Asada, H. H.; Saif, M. T. A.; Bashir, R. Three-Dimensionally Printed Biological Machines Powered by Skeletal Muscle. *Proc. Natl. Acad. Sci. U. S. A.* **2014**, *111* (28), 10125−10130.
(53) Xia, L. W.; Xie, R.; Ju, X. J.; Wang, W.; Chen, Q.; Chu, L. Y. Nano-Structured Smart Hydrogels with Rapid Response and High Elasticity. *Nat. Commun.* **2013**, *4*, 1−11.
(54) Kim, Y. S.; Liu, M.; Ishida, Y.; Ebina, Y.; Osada, M.; Sasaki, T.; Hikima, T.; Takata, M.; Aida, T. Thermoresponsive Actuation Enabled by Permittivity Switching in an Electrostatically Anisotropic Hydrogel. *Nat. Mater.* **2015**, *14* (10), 1002−1007.
(55) Takashima, Y.; Hatanaka, S.; Otsubo, M.; Nakahata, M.; Kakuta, T.; Hashidzume, A.; Yamaguchi, H.; Harada, A. Expansion−Contraction of Photoresponsive Artificial Muscle Regulated by Host−Guest Interactions. *Nat. Commun.* **2012**, *3* (1), 1270.
(56) Palleau, E.; Morales, D.; Dickey, M. D.; Velev, O. D. Reversible Patterning and Actuation of Hydrogels by Electrically Assisted Ionoprinting. *Nat. Commun.* **2013**, *4*, 1−7.

https://dx.doi.org/10.1021/acsami.0c17532
ACS Appl. Mater. Interfaces XXXX, XXX, XXX−XXX